Solid State Ionics 9 & 10 (1983) 425-430
North-Holland Publishing Company

LITHIUM INSERTION REACTIONS IN TUNGSTEN AND VANADIUM OXIDE BRONZES

Ian D. Raistrick

Department of Materials Science & Engineering
Stanford University
Stanford, CA 94305.

Thermodynamics and kinetics of the electrochemical insertion of lithium into cubic sodium tungsten bronzes and two different vanadium bronze structures have been studied. The cubic lithium sodium tungsten bronzes, $Li_yNa_xWO_3$, exhibit simple thermodynamic behavior, characteristic of a wide single phase solid solution region. The vanadium bronzes show more complex behavior, probably determined by the availability of several different kinds of crystallographic sites in these tunnel and layer structures. The solid state diffusion kinetics of all these materials are very rapid. Interfacial kinetics of the insertion of lithium from organic solvent based electrolytes have been studied using ac impedance spectroscopy, and exchange current densities obtained.

Introduction

Recent work on lithium insertion reactions into oxide materials has focused primarily on the utility of such reactions for secondary battery applications. It is evident however, that these processes constitute a large class of interesting solid-state reactions, whose thermodynamic and kinetic properties may be conveniently studied by electrochemical techniques.

In addition to lithium insertion into binary transition metal oxides, such as V_2O_5, V_6O_{13}, MoO_3 and MnO_2, a much larger class of ternary (or higher) metal oxides exists, which may be similarly intercalated by lithium to give products which may be metastable at ambient temperature, or unstable at elevated temperatures. There are also several examples of materials prepared at both low and high temperatures which differ significantly in their properties.

This paper discusses some recent results on the thermodynamics and kinetics of lithium insertion into some ternary tungsten and vanadium oxides. [1-3].

The tungsten and vanadium bronzes [4,5] are wide range non-stoichiometric compounds, in which a variable alkali metal content is compensated by the formal occurrence of two oxidation states in the transition metal ion. The formulae of the materials discussed here are M_xWO_3, $M_xV_2O_5$ and $M_{1+x}V_3O_8$, where M is an alkali metal. The x electrons donated by M may be either fully delocalised, as in the case of the tungsten bronzes, or may occupy a well-defined transition metal site as in some vanadium bronzes, or there may be a transition between localised and delocalised behavior, depending on x.

The purpose of this work was to attempt to correlate the thermodynamics and kinetics of the insertion reaction with the known structural and physical properties of these bronze families. The tungsten bronzes in particular represent a very simple example of a 3-dimensional framework structure acting as host for an inserted species. Examples of both layer and tunnel structures are found in the vanadium bronzes.

Experimental Procedures.

Samples were prepared by conventional solid state techniques. Appropriate mixtures of alkali metal tungstates or vanadates were heated with higher and lower oxides of the transition metal in sealed evacuated ampoules. The tungsten bronze single crystal samples were grown by electrolysis of molten tungstates at platinum or gold electrodes. The materials were characterised by X-ray powder diffraction and a chemical titration procedure to determine the oxidation state of the transition metal [6]. In addition, the sodium tungsten bronzes were analyzed by thermogravimetric analysis.

Electrochemical insertion of lithium was carried out using the cell:

$$Li(m)\,|\,LiAsF_6 \text{ in solvent } |\,Li_yMO_z$$

where MO_z is the transition metal oxide. A lithium reference electrode was included for the kinetic measurements. The solvent was either propylene carbonate or 2-methyl THF.

The thermodynamic data were generated by coulometric titration, in which a known quantity of charge was passed through the cell, which was then allowed to re-equilibrate, and the open circuit voltage measured. This procedure was repeated many times to generate a plot of OCV

0 167-2738/83/0000–0000/$ 03.00

versus the composition calculated from Faraday's Law. Titration curves for at least one sample from each composition were entirely reversed to confirm the efficiency and reversibility of the electrochemical reaction.

Chemical diffusion coefficients were measured on single crystal samples using galvanostatic transient techniques [7]. Total voltage excursions were limited to a few mV to ensure linearity.

A more complete picture of the kinetics of insertion from the organic solvent based electrolytes was obtained using ac techniques [8]. The sample was maintained at its OCV under potentiostatic conditions, and a small ac voltage superimposed. The electrode impedance was determined by direct sampling of cell current and voltage using a digital computer. A frequency range of 10^{-5} Hz to 50kHz was available.

Thermodynamics of Insertion

(i) Cubic Tungsten Bronzes.

The cubic bronzes have a defect perovskite structure, in which octahedral WO_6 groups are linked together through apical oxygens to form an infinite three dimensional array. The alkali metal ions occupy the large cavities at the centers of the resulting cubes (Figure 1). This structure is found for sodium concentrations of about 0.4 to 0.91. It was found that lithium could be readily inserted into cubic sodium bronzes at ambient temperature, even though the diffusion of lithium into cubic Li_xWO_3 or of sodium into Na_xWO_3 is known to be slow.

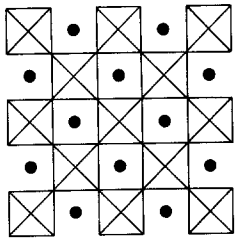

Figure 1. Crystal Structure of Cubic Na_xWO_3

Coulometric titration curves obtained on polycrystalline samples of different sodium contents are shown in Fig. 2. They have a simple shape which may be adequately explained in the following terms:

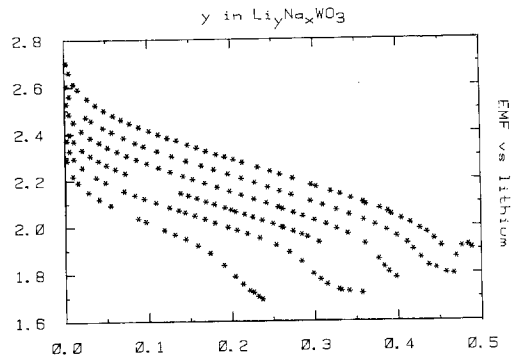

Figure 2. Coulometric Titration Curves for $Li_yNa_xWO_3$ The x-values are 0.4, 0.45, 0.49, 0.55, 0.59, 0.64 respectively, from the top of the figure.

(a) Lithium may occupy the same sites as sodium, and its maximum solubility is determined by the concentration of vacant sites. For sodium contents greater than about 0.71, negligibly small quantities of lithium may be inserted (Fig. 3), suggesting ordering of sodium atoms. According to Wiseman & Dickens [9], there are two inequivalent alkali metal sites in the structure, caused by tilting of the WO_6 octahedra. These are the larger 2(a) 12-coordinated, and the smaller 6(b) 4-coordinated sites of space group Im3. If the sodium atoms occupy the 6(b) sites exclusively, then at x = 0.75 all of the 2(a) sites will be inaccessible, and therefore unavailable to lithium. The lithium solubility would therefore fall to zero as this sodium concentration is approached.

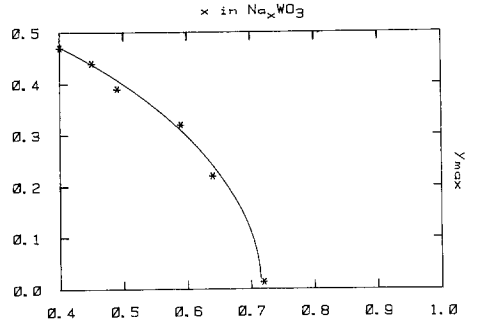

Figure 3. The Maximum Solubility of Lithium in Single Phase $Li_yNa_xWO_3$, as a Function of x.

(b) Measurement of the relative partial molar entropy of lithium by determination of the temperature coefficient of the cell voltage, indicates that the configurational entropy calculated for a distribution of lithium over (1 - x) sites is largely responsible for the simple shape of the titration curve. In addition however there is a small constant partial molar thermal entropy change, Δs_t.

$$\Delta s = - R \ln\left[\frac{y}{.37-y}\right] + \Delta s_t \qquad (1)$$

The integral entropy of insertion calculated on the basis of this model is compared to the experimental data for a sample of $Li_yNa_xWO_3$ (x = .64) in Fig. 4. The value of Δs_t for this sample was found to be -14.6 J $mole^{-1}K^{-1}$

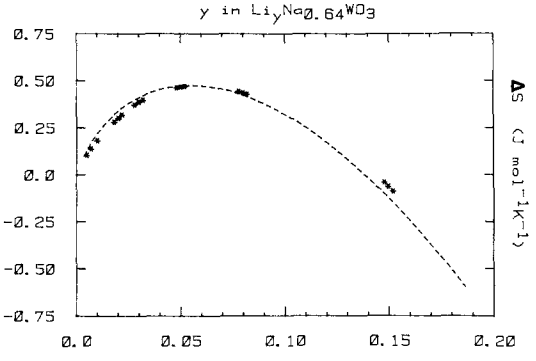

Figure 4. Integral Molar Entropy of Insertion of Lithium in $Li_yNa_xWO_3$; * experimental data; ----- calculated by integration of equation 1.

(c) The enthalpy of interaction between mobile lithiums is very small, and the principal contribution to the energy of insertion is the difference in chemical potential between electrons in the conduction band of the bronze and in lithium metal. Further, the integral free energy of formation of $Li_yNa_xWO_3$ from WO_3 and the metals, for the same total alkali metal content, i.e. (x + y), is almost independent of the x/y ratio, at least over the range x/y =1.3 to 10.7. Insertion of lithium into bronzes of low sodium content causes a slight reduction of lattice parameter and a slight distortion of the structure, leading to the occurrence of X-ray superlattice reflections, probably the same as those observed in pure Li_xWO_3[9].

(ii) Vanadium Bronzes

The insertion thermodynamics of the various vanadium bronze phases are much more complex than those of the cubic tungsten bronzes. This is caused by the more localised electronic properties, and the much more complex crystal structures of these materials. Two structures are considered here: the β-phase $M_xV_2O_5$ compounds, and the $Li_{1+x}V_3O_8$ bronze.

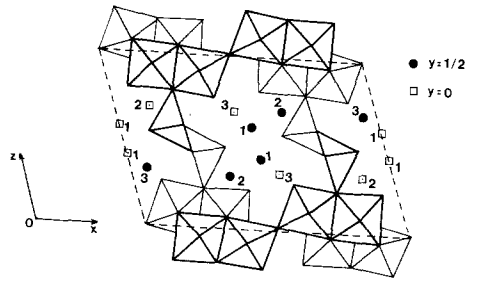

Figure 5. Crystal Structure of β-$M_xV_2O_5$

The first of these has a tunnel structure [10], Fig. 5, in which vanadium is found in 6- and 5-coordinated sites. There are several possible positions within the tunnels for the guest atoms, and the exact occupancy of the various sites depends on the concentration and size of the guest. Lithium diffuses very rapidly into both sodium and potassium beta-phase materials. Titration data for two different sodium compositions are shown in Fig. 6. Data for the potassium compound, $K_{.25}V_2O_5$, are almost identical. This is not unexpected since both sodium and potassium occupy the same sites in the tunnels (type-1 in Fig. 5). The positions of the two sudden drops in potential (single phase regions) were determined potentiostatically to occur at y = 0.40 and y = 0.73, in a sample of $Na_{.25}V_2O_5$.

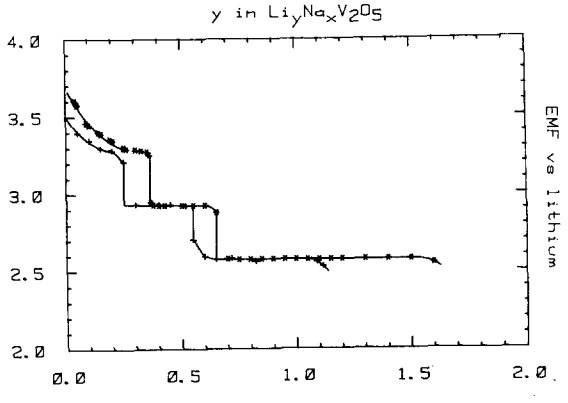

Figure 6. Coulometric Titration Curves for $Na_xV_2O_5$ (* x = 0.25, + x = .40).

The stability of phases of these compositions is most easily explained in terms of the filling of available tunnel site by lithium. X-ray data taken at these points indicate that the framework of the beta structure is still intact. The inserted lithiums may either occupy the same set of sites as the sodium or potassium ions, up to the site concentration limit of 2/3, to give $(M)^{1}_{.25}(Li)^{1}_{.41}V_2O_5$, or else they may occupy these sites until they are 1/2 filled, and then begin to occupy a second kind of site, e.g. $(M)^{1}_{.25}(Li)^{1}_{.08}(Li)^{3}_{.33}V_2O_5$. Here, the superscripts denote the kind of site occupied (Fig. 5). The second arrangement is perhaps more likely since it avoids filling more than 1/2 of the type-1 sites. This allows ordering of the alkali metals on type-1 sites displaced along the tunnel axis by b/2. If more than 1/2 of the type-1 sites are occupied then sites in the same plane must be occupied, clearly a less favorable situation.

Such an interpretation assumes, of course, that the site energies determine the phase relationships in these compounds. In fact, a sudden increase in chemical potential of lithium at (x + y) = 2/3 is also expected due to the electronic properties of the phase. The alkali metal is completely ionised in these materials and it has been argued [11] that the electron is localised on one of the three types of vanadium ion present in equal concentrations in the structure. At (x + y) =2/3, the oxidation state of 1/3 of the vanadium ions is IV, and a definite change in the chemical potential of the electrons is expected if a different type of vanadium is to be reduced, since some structural re-arrangement will occur.

Beyond (x + y) = 2/3 a two-phase region is observed, the composition of the second phase corresponding approximately to (x + y) = 1. There are several possible site filling arrangements, which might account for the stability of this phase. For example $(Li,M)^{1}_{2/3}(Li)^{3}_{1/3}V_2O_5$ & $(Li,M)^{1}_{1/3}(Li)^{3}_{2/3}V_2O_5$ are both possible. Alternative schemes involving type-2 sites are also feasible. It should be noted that single phase solid solution behavior is not seen at these higher alkali metal concentrations, presumably due to fairly strong interactions between alkali metal ions on adjacent sites. Occupancy numbers appear to be either 1/2 or 1, and intermediate fillings are not favorable.

Lithium is also mobile in the pure lithium containing phase $Li_yV_2O_5$, as suggested by Gendell, Cotts & Sienko [12], on the basis of NMR results. The titration curve for this material is very complex, and significantly different from that of the sodium and potassium bronzes. It is also different from the reported phase relations for the lithium bronzes prepared at high temperatures.

The phase $Li_{1+y}V_3O_8$ has a quite different structure from that of the beta-phase materials. It is a layer structure consisting of ribbons of 5- & 6-coordinated vanadiums, the oxygen atoms of which are linked by lithiums [13] (Fig. 7).

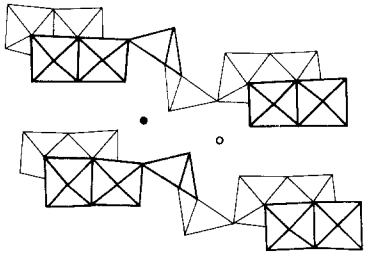

Figure 7. Crystal Structure of $Li_{1+y}V_3O_8$.

This compound has previously been investigated by Schollhorn et al. [14], who studied primarily its ion exchange properties in aqueous solutions. The kinetics of lithium insertion from aprotic electrolytes, however are also remarkably rapid, and about two lithiums may be accommodated in the structure, beyond those initially present due to the preparation (Fig. 8). The data shown here differ considerably from results of phase relations obtained at high temperatures. Since this is a layer structure, rather than a framework, it is possible that solvent interactions are important here. Schollhorn et al. have shown that water may co-intercalate this material with considerable increase in lattice parameter.

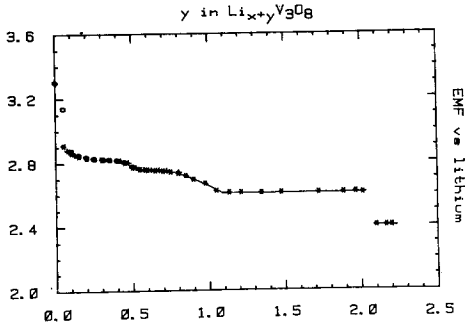

Figure 8.Coulometric Titration Data for $Li_{x+y}V_3O_8$ (x = 1.5).

Kinetics of the Insertion Process.

Insertion reactions of this type are in general expected to be controlled by the rate of solid state diffusion. If diffusion is sufficiently rapid however, than interface kinetics may become important. A detailed study of the chemical diffusion of lithium into single crystal samples of the cubic sodium tungsten bronzes has been undertaken and the results published elsewhere [2]. Chemical diffusion coefficients were found to be very high at ambient temperatures (about 10^{-7} cm^2/s at low lithium concentrations). In order to investigate the role of interface kinetics in the insertion process from organic solvents, an ac study was undertaken, and preliminary results are reported here.

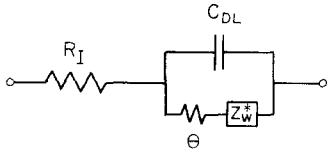

Figure 9. Equivalent Electrical Circuit for Insertion Reactions.

The overall kinetic scheme for a small amplitude ac perturbation in the absence of specific adsorption is expected to be equivalent to that of the Randles circuit of Fig. 9. θ is the interfacial reaction resistance:

$$\theta = \frac{RT}{nI_0F} \qquad (2)$$

where I_0 is the exchange current density, and n is the charge number of the electroactive species. C_{dl} is the capacitance of the double layer and Z_W is the impedance due to diffusion [8]:

$$Z_W = (1-j)\frac{V_m(dE/dy)}{nFs\sqrt{2\omega D}} \qquad (3)$$

Here, V_m is the molar volume, s is the surface area and D is the chemical diffusion coefficient. R_i is the series resistance due to electrolyte, leads etc.

Typical complex impedance plots for the insertion of lithium into single crystal Na_xWO_3 from 1M $LiAsF_6$ in propylene carbonate are shown in Fig. 10. The data were obtained at the same temperature (21°C), but at different concentrations of inserted lithium in the

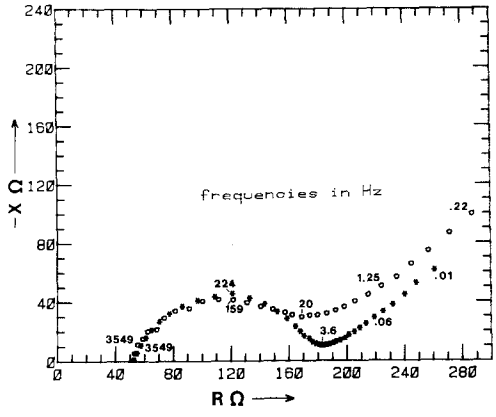

Figure 10. Complex Impedance Data for Li_yNa_x WO_3 (x = 0.64) O E = 1.85 V; * E = 2.00 V (versus lithium).

electrode. At low frequencies straight lines, inclined at 45° to the real axis, and characteristic of diffusion, are seen. At frequencies above about 1Hz, circular arcs, rather than the semi-circle predicted by the Randles circuit, are seen. The separation between the arc and the straight line is less clear at higher lithium concentrations due to the slower diffusion kinetics in the solid. The diameter of the arc on the real axis is assumed to be equal to the interfacial reaction resistance. This quantity was determined at four different electrode potentials (i.e. four different concentrations of lithium), as a function of temperature. As expected, the interfacial reaction resistance decreased with increasing temperature. The logarithms of the calculated exchange current densities are plotted versus reciprocal absolute temperature in Fig 11. As can be seen, the activation enthalpy is constant, within experimental error, and equal to about 50 kJ/mole. The independence of the activation enthalpy from the electron concentration might suggest that the rate determining step of the heterogeneous interface reaction is associated with the ion rather than the electron transfer.

Conclusions.

Lithium may be rapidly inserted into a number of non-stoichiometric oxide bronze phases from organic solvent based electrolytes at ambient temperatures. A number of different structures have been investigated, including the three dimensional framework of the defect perovskite

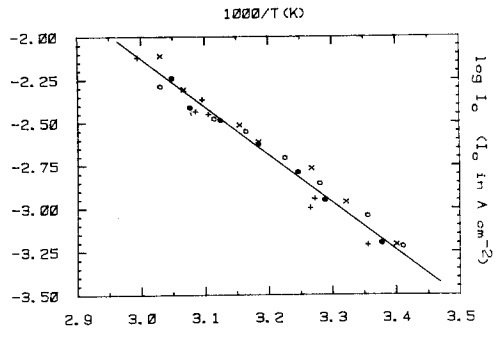

Figure 11. Log of Exchange Current Densities as a Function of Reciprocal Temperature for Different Compositions of $Li_yNa_xWO_3$ (x = 0.64). + E = 2.25 V; o E = 2.14 V; • E = 2.00 V; x E = 1.85 V (versus lithium).

structure, the tunnel structure of the beta vanadium bronzes, and the layer structure of $Li_{1+y}V_3O_8$.

All three classes of material show wide ranges of single phase solid solution behavior. The cubic tungsten bronzes show the simplest behavior as there is only one kind of site for the inserted species, and their electronic properties vary smoothly with alkali content. The free energy of insertion can be adequately modelled using a free electron gas approach, and a system of non-interacting lithium ions distributed over available sites.

The beta vanadium bronzes also show an initial domain of extended solid solubility, the limits of which can be explained either in terms of ion site energies or electronic properties. At higher lithium concentrations, geometric considerations imply strong interactions between alkali ions, leading to multi-phase behavior and sites are either 1/2 or fully occupied. These phases are metastable with respect to lattice rearrangements. The tungsten bronzes on the other hand are stable with respect to lattice reconstruction, and at high temperatures, only an irreversible disordering of the lithium and sodium atoms is observed.

The layer structure material $Li_{1+y}V_3O_8$ also forms metastable insertion compounds at ambient temperature with the same type of solid solution behavior at lower lithium contents, and biphasic behavior at higher.

The diffusion kinetics of the insertion reactions are all rapid, and diffusion coefficients around 10^{-7} cm^2/s are common. In this kind of system, interface kinetics can also be important and complex impedance spectroscopy has allowed the measurement of exchange current densities on single crystals of the cubic tungsten bronzes. It has been found that the interface kinetics are thermally activated, as expected, and that the rate of the heterogeneous reaction is essentially independent of the concentration of lithium present in the electrode.

Both the vanadium bronze systems are potentially attractive positive electrode materials for lithium cells, having high potentials versus lithium, rapid diffusion kinetics and reversible insertion reactions. They are not however, metallic conductors over their entire compositional ranges, and the addition of an electronically conducting phase appears necessary to fully utilise their capacity.

References

[1] I. D. Raistrick, A. J. Mark & R. A. Huggins, Sol. St. Ionics 5, 351 (1981).
[2] A. J. Mark, I. D. Raistrick & R. A. Huggins, J. Electrochem. Soc. 130, 776 (1983).
[3] I. D. Raistrick & R. A. Huggins, Mater. Res. Bull. (To be published).
[4] P. G. Dickens & P. J. Wiseman in "International Review of Science: Inorganic Chemistry" Series 2, Vol. 10. L. E. J. Roberts (ed.) p 211. Butterworth's, London (1975).
[5] P. Hagenmuller in "Pergamon Texts in Inorganic Chemistry" Vol. 1. Pergamon Press, Oxford (1973).
[6] C. Choain & F. Marion. Bull. Soc. Chim. France. 212 (1963).
[7] W. Weppner & R. A. Huggins. J. Electrochem. Soc. 124, 1509 (1977).
[8] C. Ho, I. D. Raistrick & R. A. Huggins. J. Electrochem. Soc. 127, 343 (1980).
[9] P. J. Wiseman & P. G. Dickens. J. Sol. State. Chem. 17, 91 (1976).
[10] A. D. Wadsley. Acta Cryst. 8, 695 (1955).
[11] J. B. Goodenough. J. Sol. State Chem. 1, 349 (1970).
[12] J. Gendell, R. M. Cotts & M. J. Sienko. J. Chem. Phys. 37, 220 (1962).
[13] A. D. Wadsley. Acta Cryst. 10, 261 (1957).
[14] R. Schollhorn, F. Klein-Reesink & R. Reimold. J. C. S. Chem. Comm. 398 (1979).

Acknowledgement

This work was supported by the United States Department of Energy under subcontracts LBL 45030110 & LBL 4519410.